Effects of RbI and CuBr$_2$ addition to CH$_3$NH$_3$PbI$_{3-\delta}$Cl$_\delta$ photovoltaic devices

Naoki Ueoka, Takeo Oku and Atsushi Suzuki

Department of Materials Science, The University of Shiga Prefecture,
2500 Hassaka, Hikone, Shiga 522-8533, Japan
Phone: +81-749-28-8369   E-mail: oh21nueoka@ec.usp.ac.jp

Abstract

Additive effects of RbI and CuBr$_2$ to CH$_3$N$_3$PbI$_{3-\delta}$Cl$_\delta$ photovoltaic devices were investigated. Grains sizes of the perovskite crystals were increased by excess RbI addition. Amount of CuBr$_2$ addition was investigated and optimized for the cells. As a result, the best conversion efficiency was obtained by a small amount of addition of RbI and CuBr$_2$. The energy band gap was increased by Cu substitution, which was confirmed by first-principles calculations.

1. Introduction

CH$_3$NH$_3$PbI$_{3-\delta}$Cl$_\delta$-type compounds have been widely studied [1]. These perovskite compounds can be formed by reacting a mixture of the precursors CH$_3$NH$_3$I and PbCl$_2$ in a 3:1 molar ratio. In our previous work, photovoltaic properties of perovskite solar cells were improved by adding CuX (X = I, Br, or Cl) to the perovskite precursors through the use of an air-blowing method [2].

The purpose of the present study is to fabricate and characterize CH$_3$NH$_3$PbI$_{3-x}$Cl$_x$ photovoltaic devices added with RbI and CuBr$_2$. Elements with ionic radii smaller than CH$_3$NH$_3^+$ (2.17 Å) were added to the solution to compensate for the lattice distortion caused by Cu substitution at Pb sites. Thus, we discuss the effects of RbI and CuBr$_2$ addition. The electronic structures were also investigated by first-principles calculations.

2. Experimental

The 0.15 M TiO$_2$ precursor solution was spin-coated on the FTO substrate and the coated substrate was then annealed at 125 °C for 5 min. Then, the 0.30 M TiO$_x$ precursor solution was spin-coated on the TiO$_2$ layer and the resulting substrate was annealed at 125 °C for 5 min. The process for forming the 0.30 M precursor layer was performed twice. Then, the FTO substrate was sintered at 550 °C for 30 min to form a compact TiO$_2$ layer. The mesoporous TiO$_2$ layer was spin-coated on the compact TiO$_2$ layer. The resulting cell was heated at 125 °C for 5 min and then annealed at 550 °C for 30 min. The Perovskite solutions with 1–2% RbI and 1–2% CuBr$_2$ of PbCl$_2$ molar were then introduced into the TiO$_2$ mesopores by spin coating, followed by annealing at 140 °C for 10 min. Then, spiro-OMeTAD was spin-coated on the perovskite layer. Finally, gold (Au) electrodes were evaporated as top electrodes using a metal mask for the patterning.

3. Results and discussion

J–V characteristics under illumination recorded in the reverse scan of the perovskite cells are shown in Fig. 2. Measured photovoltaic parameters of the present perovskite cells are summarized in Table 1. The CuBr$_2$ + RbI cell provided a short-circuit current density (J_{SC}) of 22.3 mA cm^{-2}, an open-circuit voltage (V_{OC}) of 0.925 V, a fill factor (FF) of 0.690, and a conversion efficiency (η) of 14.2%. The sheet resistance (R_S) was increased to 5.95 Ω cm^2 by excess RbI addition. The J_{SC} was decreased to 17.6 mA cm^{-2} by excess CuBr$_2$ addition.

SEM images of the perovskite cells are shown in Fig. 3. The perovskite grain sizes were increased by excess RbI addition, which resulted in increase in R_S. The poor perovskite film was formed by excess CuBr$_2$ addition due to the lattice distortion. However, the perovskite grains slightly grew by 2% excess RbI addition to CuBr$_2$ added cell.

Electronic structures at HOMO and LUMO of the present perovskite crystals were calculated, as shown in Fig. 4. The electric charge distribution was changed by interaction between Rb and Cu, which influences the carrier transport properties. Total density of states with up-α spin for the present perovskite structures are shown in Fig. 5. The electronic structures of CH$_3$NH$_3$PbI$_3$ mainly derive from the electronic state of the PbI$_6$ octahedron unit, and the level of the energy band is comprised of Pb 6s, 6p and I 5p orbits. The energy level at the HOMO is a σ anti-binding state between Pb 6s and I 5p orbits, and the LUMO is a mixed σ or π anti-binding state between Pb 6p and I 5s or 5p orbits. Therefore, substitution of other elements at Pb sites influences the HOMO and LUMO levels. The DOS at the HOMO was greatly increased by Cu substitution but not influenced by Rb. Hence, the 3d orbital of Cu influences the energy level at HOMO and contributes to an increase in carrier generation.
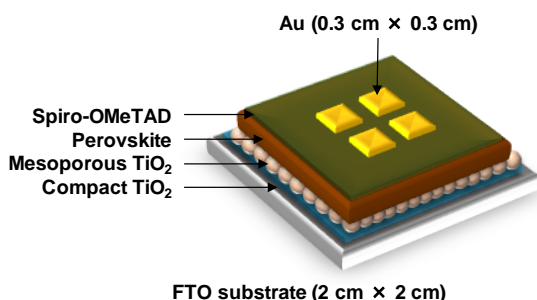

Au (0.3 cm × 0.3 cm)
Spiro-OMeTAD
Perovskite
Mesoporous TiO$_2$
Compact TiO$_2$
FTO substrate (2 cm × 2 cm)

Fig. 1. Structure of the perovskite cell.
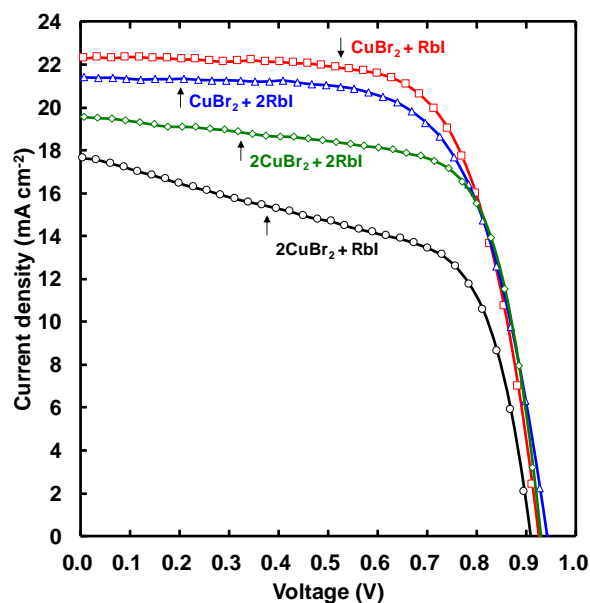
Fig. 2. *J–V* characteristics of the present perovskite cells.
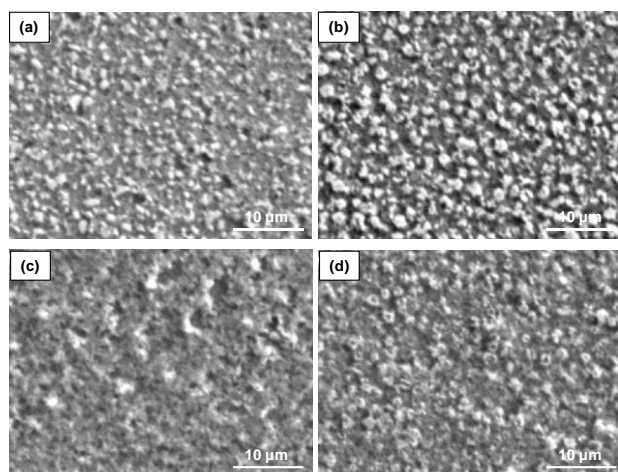
Fig. 3. SEM images of (a) CuBr$_2$ + RbI, (b) CuBr$_2$ + 2RbI, (c) 2CuBr$_2$ + RbI, and (d) 2CuBr$_2$ + 2RbI perovskite cells.
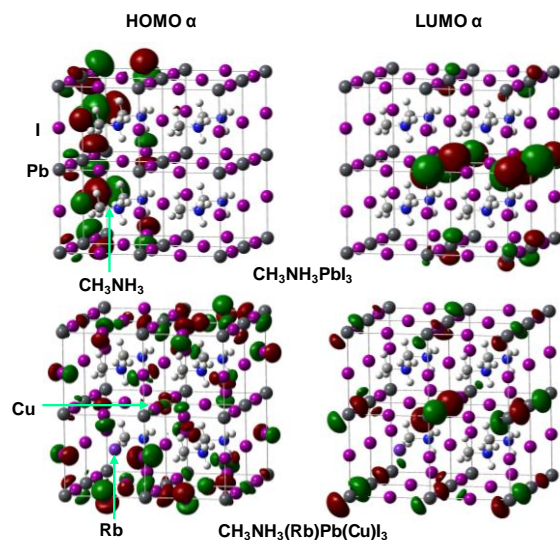

Fig. 4. Electronic structures at HOMO and LUMO of the perovskite structures.
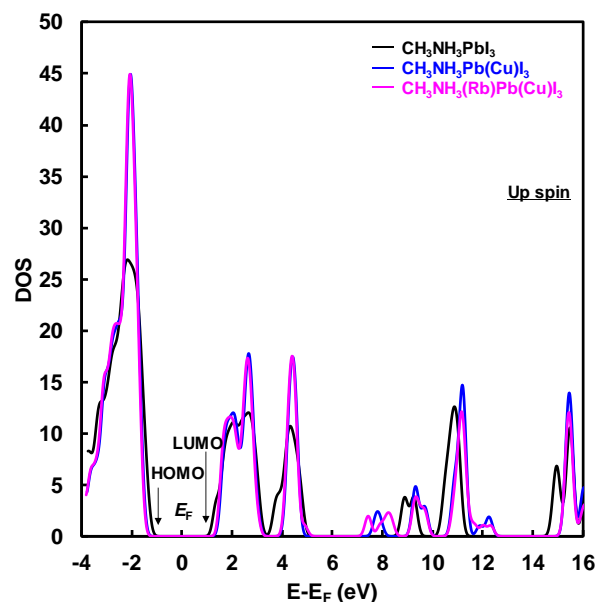

Fig. 5. Total density of states of the present perovskite structures.

Table 1. Photovoltaic parameters of the perovskite solar cells.

Cells	J_{SC} (mA cm^{-2})	V_{OC} (V)	FF	η (%)	η_{ave} (%)	R_S (Ω cm^2)	R_{Sh} (Ω cm^2)
CuBr$_2$ + RbI	22.3	0.925	0.690	14.2	13.8	4.77	4660
CuBr$_2$ + 2RbI	21.4	0.941	0.672	13.5	13.4	5.95	2690
2CuBr$_2$ + RbI	17.6	0.909	0.600	9.6	9.0	4.93	177
2CuBr$_2$ + 2RbI	19.6	0.928	0.704	12.8	12.2	4.19	454

References
1. L. Cojocaru, S. Uchida, D. Matsubara, H. Matsumoto, K. Ito, Y. Otsu, P. Chapon, J. Nakazaki, T. Kubo and H. Segawa, Chem. Lett. **45** (2016) 884.
2. H. Tanaka, Y. Ohishi and T. Oku, Jpn. J. Appl. Phys. **57** (2018) 08RE10.